УДК 004.932.2

O. Buchko

SHAPE-BASED CLASSIFICATION OF RADIOLOGICAL IMAGES

The paper presents the results of an investigation of methods for providing categorization between normal and pathological brain structures from magnetic-resonance (MR) images based on a shape description. The shape description techniques have been applied to two groups: one group of 30 healthy controls and second group of 17 patients with brain pathology.

Shape description in medical imaging has become an increasingly important research field in recent years. Fast and high-resolution image acquisition methods like Magnetic Resonance (MR) imaging produce very detailed cross-sectional images of the human body which are then investigated by clinicians and other experts. Shape description is a post-processing operation which abstracts quantitative descriptions of anatomical object shapes.

Clinicians and other experts are particularly interested in quantification of deformations of the brain for special diseases such as Alzheimer's disease, vascular dementia, Huntington's disease, Parkinson's disease, and distinguishing between normals and abnormals. This information is usually obtained manually by the analysis of the images.

In this work we analyze shape of brain structures by using different description techniques based on either shape boundary information or boundary plus interior content. The goal of this paper is to test and demonstrate capability of the proposed shape description techniques to discriminate between normal and pathological conditions.

The shape description techniques have been applied to two groups: one group with only subtle deformations of the white brain matter, a group of 30 healthy controls, and second group with severe deformations of the white matter, a group of 17 patients with pathology.

Shape description techniques

There are many shape description techniques have been proposed in the literature [1–5]. Here we recall descriptors that we used for shape analysis of brain structures. Assuming that the contour is defined in parametric form $c(l) = (x(l), y(l))$, every point $(x_0, y_0)...(x_{N-1}, y_{N-1})$ of the contour c of the object can be represented by taking the arc length l as a parameter with $0 \le l \le L$, where L is the length of the contour.

Common simple shape descriptors of an object X are perimeter, area, compactness.

Compactness, determined by using the perimeter $P(X)$ and area $A(X)$ of an object X, defined as $C(X) = P(X)^2 / A(X)$ which measures roundedness of a shape how close an object is to the circle. The value of compactness is minimal for circular shape ($4\pi \approx 12.57$ for circle) that encloses a given area with the shortest perimeter. The value increases with increasing shape complexity.

Shape of an object can be represented by its bending energy, defined as the energy necessary to bend a rod to a desired shape and is obtained as the sum of squared contour curvature $k(l)$ over the contour having length L:

$$B(X) = \frac{1}{L}\sum_{i=0}^{N-1} k(l_i)^2 \ , \qquad (1)$$

where $k(l)$ given by

$$k(l) = \frac{\dot{x}(l)\ddot{y}(l) - \dot{y}(l)\ddot{x}(l)}{(\dot{x}(l)^2 + \dot{y}(l)^2)^{3/2}} \qquad (2)$$

The concept of moments used to analyze statistical distributions can also be used to achieving invariant description respect to translation, rotation, and scaling. The contour-based moments are given by

$$m_{pq}^c = \sum_{i=0}^{N-1} \left(x(l_i)\right)^p \left(y(l_i)\right)^q \qquad (3)$$

The central contour-based moments can be obtained by

$$\mu_{pq}^c = \sum_{i=0}^{N-1} \left(x(l_i) - \overline{x}(l_i)\right)^p \left(y(l_i) - \overline{y}(l_i)\right)^q \ ,$$

$$\text{where } \overline{x}(l_i) = \frac{m_{10}^c}{m_{00}^c} \text{ and } \overline{y}(l_i) = \frac{m_{01}^c}{m_{00}^c} \qquad (4)$$

m_{00}^c correspond with the length of the object boundary.

The scale invariant central contour-based moments will be defined as

$$\eta_{pq}^c = \mu_{pq}^c \mu_{oo}^{c\ -\beta}, \text{ where } \beta = p + q + 1 \qquad (5)$$

A set of invariant moments with respect to translation, rotation, and scaling can be obtained from second- and third-order moments. Some examples are:

© *O. Buchko*, 2009

$$\phi_1 = \eta_{20}^c + \eta_{02}^c \quad \phi_2 = (\eta_{20}^c - \eta_{02}^c)^2 + 4\eta_{11}^{c\,2} \qquad (6)$$
$$\phi_3 = (\eta_{30}^c - 3\eta_{12}^c)^2 + (3\eta_{21}^c - \eta_{03}^c)^2$$

The eccentricity ε of an object ranges from 0 for circular object to 1 for a straight line and can be measured as

$$\varepsilon = \frac{(\mu_{20}^c - \mu_{02}^c)^2 + 4\mu_{11}^{c\,2}}{(\mu_{20}^c + \mu_{02}^c)^2} \qquad (7)$$

The fractal dimension **is often considered as a** parameter **describing morphological complexity** of object. The fractal dimension value indicates how object is reflected within scaling and self-similarity geometrical properties; it is the relationship between measured quantity (perimeter, area, volume) and the scale at which that quantity is measured. In recent years fractal analysis has been applied to studying of a wide range of objects in biology and medicine, for example to diagnosing blood cells [8], to detecting micro-calcification in mammograms [6], small peripheral lung tumors [7], to analyzing bones [10]. Fractal analysis is especially useful while quantifying human brain, with of its highly complex structure. It has been used in quantifying shape of the brain [11–20].

A wide variety of fractal dimension definitions have been proposed [21–27], among them are self-similarity dimension, Hausdorff dimension, Minkowski dimension, packing (Tricot) dimension, box-counting dimension, divider dimension and others. Fundamental to most definitions of dimension is the idea of measurement N_δ at scale δ. For each δ, a fractal object has been measured in a way that ignores irregularities of size (length, area, volume, etc.) less than δ, and then we see how these measurements behave when $\delta \to 0$.

For example, if object X is a plane curve then measurement $N_\delta(X)$ might be the number of steps, self-similar pieces into which an object can be divided by length δ following direction *X*. The dependence of $N_\delta(X)$ as $\delta \to 0$ can be mathematically expressed as power law of the form

$$N_\delta(X) \sim const \cdot \delta^{-D_G} \qquad (8)$$

Where *const* is a constant and D_G is a fractal dimension of our object *X*. Equivalently

$$D_G(X) = \lim_{\delta \to 0} \frac{\log N_\delta(X)}{-\log \delta} \qquad (9)$$

Assuming the limit exists.

In our investigation for calculation of fractal dimension two methods have been used box-counting dimension and divider dimension.

The box-counting dimension is one of the most widely used fractal dimensions. This dimension is largely popular due to its relative easiness of calculation. The box-counting method works by covering image with δ-mesh boxes and then evaluating how many boxes are needed to cover fractal object completely. Repeating this measurement with different sizes of boxes δ will result into logarithmical function of box size $\log(1/\delta)$ and number of boxes needed to cover object ($\log N$). The box-counting fractal dimension D_B of the object can be estimated as the angle of slope of the line observed in the plot of $\log N$ as respects $\log(1/\delta)$ which correspond to Richardson plot [21] that can be estimated from a linear regression defined by $\log N = D_B \cdot \log(1/\delta) + const$.

The divider dimension (some authors also called it compass, ruler dimension, hand and dividers, structured walk technique, yardstick method) [22, 25, 27, 28] is based on curve perimeter estimation using δ– «step» of different size. This dependence can be mathematically expressed as relation $P(X) \approx \delta^s$, where *P(X)* is the perimeter of the object X, δ is a step size and s is the angle of slope of the line observed in the plot of $\log(P(X))$ as respects $\log(\delta)$ which correspond to the Richardson plot [21]. The angle of slope of this line can be estimated from a linear regression defined by $\log(P(X)) = s \cdot \log(\delta) + const$. This angle of slope is connected to the divider fractal dimension as $D_{div} = 1 - s$.

Investigation

The shape description techniques have been applied to two groups: one group of 30 healthy controls with only subtle deformations of the white brain matter and second group of 17 patients with pathology, with severe deformations of the white matter.

For investigation the axial T2-weighted MR image data sets were used. Depending on the individual patient each set consisted of 22–24 of brain slices (images), each slice being 512x512 pixel matrix. Shape description measurements (area, perimeter, compactness, Feret's diameter, bending energy, eccentricity, invariant moment, box-counting fractal dimension, divider fractal dimension) were performed on an intermediate slice where the brain is the most circular-shaped and has maximum expansion which is usually between slices 13 and 16, in most cases it is 15 of each MR image data sets. A combination of the following techniques helps to achieve a segmentation of regions and a detection boundary of regions: thresholding, morphological open, labeling (based on region growing method), finding the largest region, boundary tracing.

From figures in Fig.1(a, b, c) it becomes obvious that perimeter of the white brain matter, compactness of the white brain matter and invariant moment (combination of scale invariant central moments

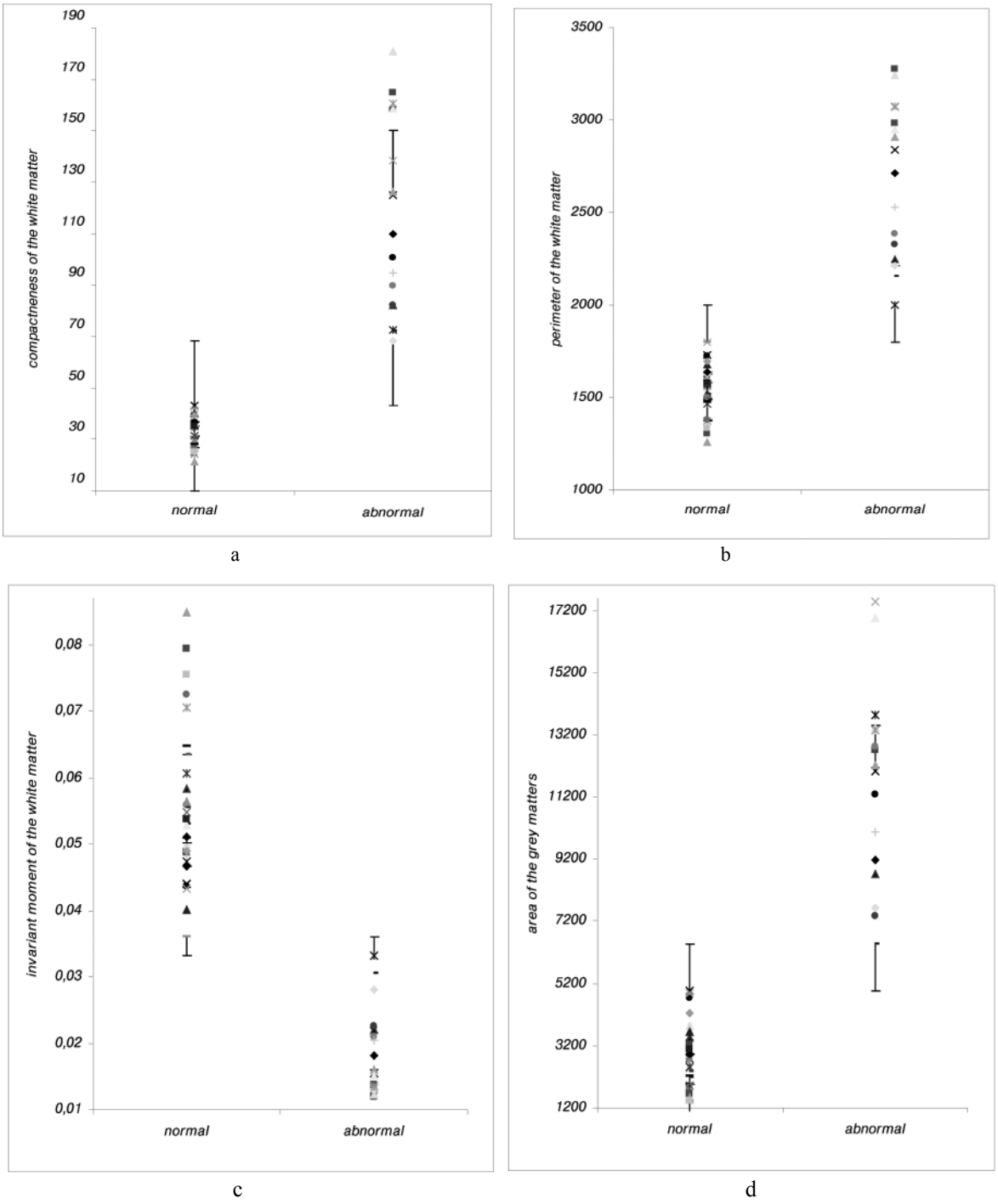

Fig. 1. (a) compactness, (b) perimeter, (c) invariant moment of the white brain matter, (d) area of the grey brain matter of the first and second groups of patients.

given in Eq. (6)) of the white brain matter indicate quite clear demarcation between two groups of patients: perimeter values for the first group range between [1258; 1796], for second group range between [2000; 3276]; compactness values for the first group range between [21.42; 43.26], for second group range between [68.53; 180.93]; invariant moment values for the first group range between [0.03606; 0.08479], for second group range between [0.01192; 0.0332].

In terms of absolute values, perimeter, compactness of the white brain matter measurements yield overall highest values and invariant moment of the white brain matter measurements are lowest values for second group of patients than for the first one.

Area, Feret's diameter, bending energy and eccentricity of the white brain matter measurements show no clear demarcation for both groups of patients. But difference of area of the white brain matter and area of the white and grey brain matters

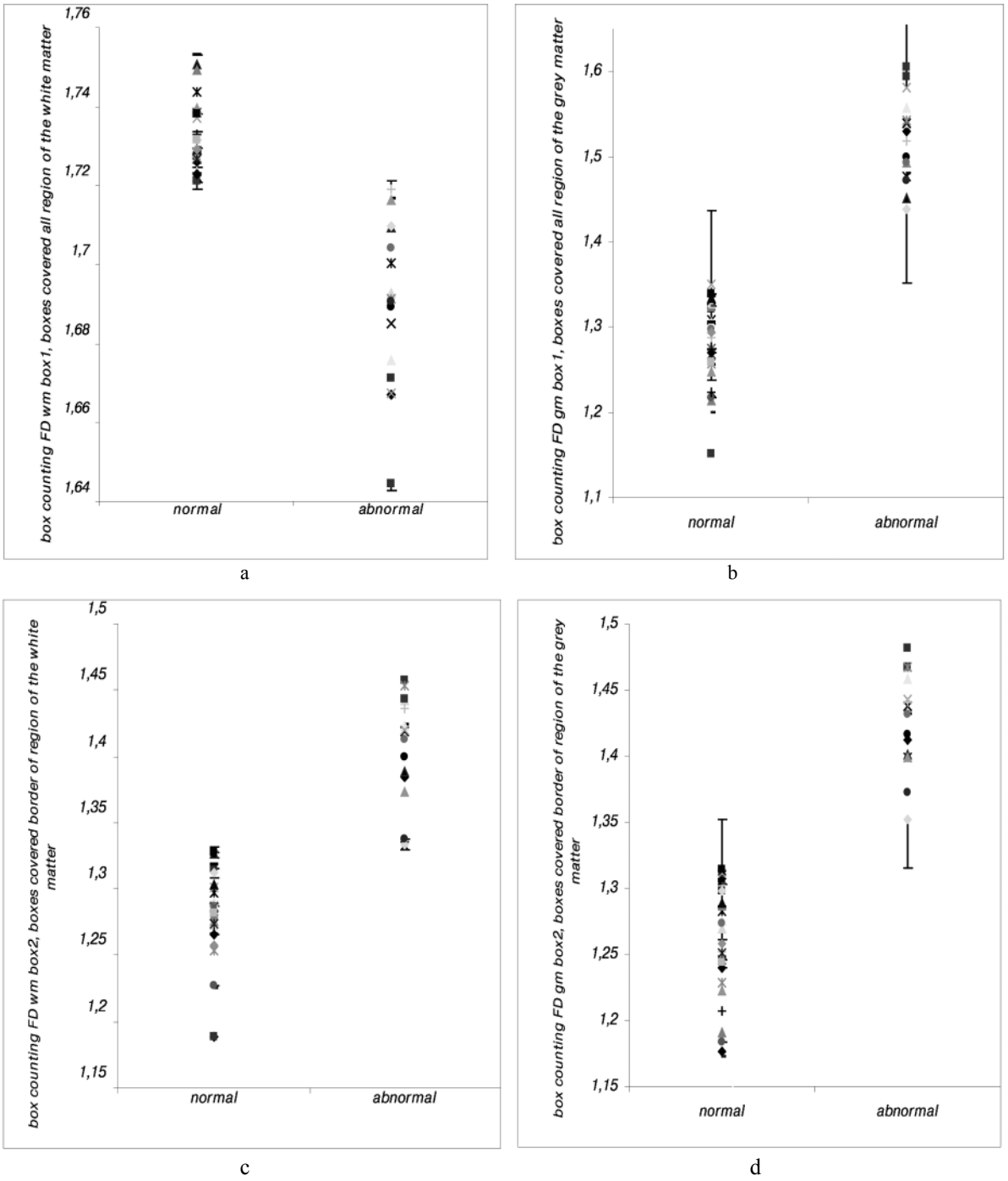

Fig. 2. Box counting fractal dimension a)counting boxes that covered all region of the white brain matter of the first and second groups of patients b) counting boxes that covered all region of the grey brain matter of the first and second groups of patients c) counting boxes that covered border of region of the white brain matter of the first and second groups of patients d) counting boxes that covered border of region of the grey brain matter of the first and second groups of patients

(equals area of the grey matter), illustrated in Fig. 1(d), indicates quite clear demarcation between two groups of patients: the values for the first group range between [1407; 4975] while for patients from second group lie in between [6473; 20566].

The fractal dimension measurements of FD_{wm_box1} (box counting fractal dimension, counting boxes that covered all region of the white matter), which are illustrated in Fig. 2.(a) show a slightly clear demarcation between two groups of patients: the values for the first group range between [1.72123; 1.75315] while for patients from second group lie in between [1.64462; 1.71917]. This result can be explained, first of all, by the modification of classical measurements that have been performed (classical counting boxes that covered border of region); sec-

ondly, all patients are chosen as general, patients have not been specially selected for their qualities, such parameters as age, gender, genetics have not been taken into account; thirdly, in the second group that we investigated consisted of patients with different neurological diseases which are closely related to pathology of the brain structures.

Fig. 2(b, c, d) and Fig. 3 show that the other fractal dimension measurements indicate quite clear demarcation between two groups of patients:

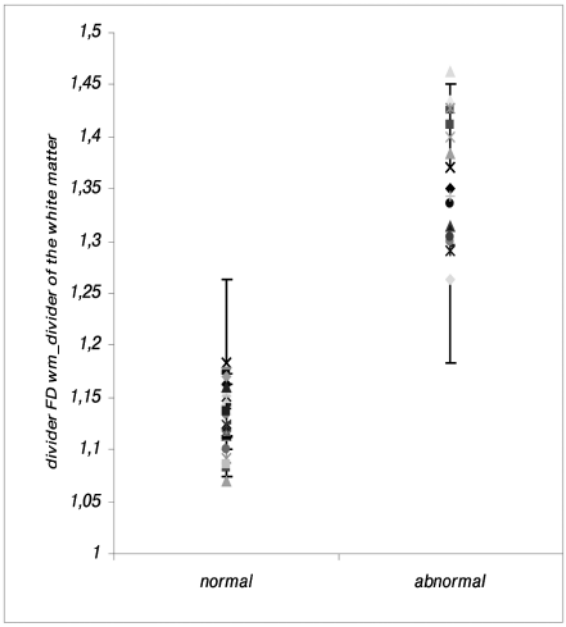

Fig. 3. Divider fractal dimension of the white brain matter of the first and second groups of patients

FD_{gm_box1} (box counting fractal dimension, counting boxes that covered all region of the grey matter): the values for the first group range between [1.15068; 1.35013], for second group range between [1.43807; 1.60475].

FD_{wm_box2} (box counting fractal dimension, counting boxes that covered border of region of the white matter): the values for the first group range between [1.18847; 1.3279], for second group range between [1.33255; 1.45707].

FD_{gm_box2} (box counting fractal dimension, counting boxes that covered border of region of the grey matter): the values for the first group range between [1.13012; 1.31473], for second group range between [1.35206; 1.48182].

$FD_{wm\_divider}$ (divider fractal dimension of the white brain matter): the values for the first group range between [1.06917; 1.18304], for second group range between [1.2635; 1.4619].

The most important observation is the all fractal dimension measurements yield overall lowest values for patients from first group, and overall highest values for patients from second group with a single exception of FD_{wm_box1} (box counting fractal dimension, counting boxes that covered all region of the white matter) fractal dimension measurements. The reasons that FD_{wm_box1} fractal dimension measurements yield distinctively different results discussed above.

Conclusions

In this paper we are currently investigating methods for providing categorization between normal and pathological brain structures from MR images based on a shape analysis. Shape description measurements for the two groups of the brain data sets were performed, a first group of 30 healthy controls, and second group with severe deformations of the white matter, a group of 17 patients with pathology.

The perimeter, compactness and invariant moment of the white brain matter have shown potential to categorize the investigated cases into shapes of low and high complexity (normal and abnormal cases). The (FD_{gm_box1}, FD_{wm_box2}, FD_{gm_box2}, $FD_{wm\_divider}$) fractal dimension measurements also showed a potential for providing categorization.

Highest values of perimeter and compactness of the white brain matter have been observed for data of high complexity (second investigated group) and lowest values for data of low complexity (first investigated group). Lowest values of invariant moment of the white brain matter coincided more with data of high complexity (second investigated group) and highest values for data of low complexity (first investigated group). Highest values of fractal dimension have been observed for data of high complexity, lowest values of fractal dimension coincided more with data of low complexity. From this the following observation can be made: perimeter, compactness and invariant moment of the white brain matter and (FD_{gm_box1}, FD_{wm_box2}, FD_{gm_box2}, $FD_{wm\_divider}$) fractal dimension measurements are intrinsically, but in most cases not directly (invariant moment directly) related to shape properties, and are capable of discrimination between normal and abnormal shapes (low and high complexity).

1. Schnabel J. Shape description methods for medical images / J. Schnabel; Technical report TR/95/12, London, 1995.
2. Zhang D. Review of shape representation and description techniques. / D. Zhang, G. Lu; Pattern Recognition vol. 37, p. 1–19, 2004.
3. Loncavic S. A survey of shape analysis techniques. / S. Loncavic; Patter Recognition, vol. 31(8), p. 983–1001, 1998.
4. Sonka M. Image processing, analysis and machine vision / M. Sonka, V. Hlavac, R. B.; Chapman and Hall, 1993, ISBN-13: 9780412455704. http://css.engineering.uiowa.edu/%7Edip/LECTURE/lecture.html
5. Aguado A. S. Feature extraction and image processing / A. S. Aguado, M. S. Nixon; Newnes, Oxford, First edition 2002, ISBN: 0-7506-5078-8.

6. Caldwell C. B. Characterisation of mammographic parenchymal pattern by fractal dimension. / C. B. Caldwell, S. J. Stapleton, D. W. Hodsworth, et al. // Physics in Medicine and Biology, vol. 35(2), p. 235–247, 1990.
7. Mihara N. The usefulness of fractal geometry for the diagnosis of small peripheral lung tumors. / N. Mihara, K. Kuriyama, S. Kido, et al.// Nippon Igaku Hoshasen Gakkai Zasshi, vol. 58(4), p. 148–151, 1998.
8. Kotarski W. Shape analysis of blood cells based on fractal dimension. / W. Kotarski, S. Widuch // Journal of Medical Informatics and Technologies, vol. 2, p. MI177-182, 2001.
9. Webber R. L. Predicting osseous changes in ankle fractures. / R. L. Webber, T. E. Underhill, R. A. Horton, et al. // IEEE, Engineering in Medicine and Biology Magazine, vol. 12(1), p. 103–110, 1993.
10. Feltrin G P. Bone fractal analysis. / G P. Feltrin, R. Stramare, D. Miotto, et al. // Current Osteoporosis Reports, vol. 2, p. 53–58, 2004.
11. Bullmore E. Fractal analysis of the boundary between white matter and cerebral cortex in magnetic resonance images: A controlled study of schizophrenic and manic-depressive patients. / E. Bullmore, M. Brammer, I. Harvey, et al. // Psychological Medicine, vol. 24 (3), p. 771–781, 1994.
12. Cook M. J. Fractal description of cerebral cortical patterns in frontal lobe epilepsy. / M. J.Cook, S. L. Free, M. R. A. Manford, et al. // European Neurology, vol. 35 (6), p. 327–335, 1995.
13. Schnabel J. Fractal feature analysis and classification of MS lesions. / J. Schnabel, L. Wang, D. Rueckert, S. Arridge // Computer Assisted Radiology, Berlin, p. 21–24, 1995.
14. Free S. L. Three-dimensional fractal analysis of the white matter surface from magnetic resonance images of the human brain. / S. L. Free, S. M. Sisodiya, M. J. Cook, et al. // Oxford University Press, Cerebral Cortex, vol. 6 (6), p. 830–836, 1996.
15. Thompson P. M. Three-dimensional statistical analysis of sulcal variability in the human brain. / P. M. Thompson, C. Schwartz, R. T. Lin, et al. // The Journal of Neuroscience, vol. 16 (3), p. 4261–4274, 1996.
16. Rybaczuk M. Fractal analysis of adults cerebellum surface NMR observations. / M. Rybaczuk, A. Kedzia // Folia Morphologica (Warszawa), vol. 55(4), p. 431–433, 1996.
17. Blanton R. E. Mapping cortical asymmetry and complexity patterns in normal children. / R. E. Blanton, J. G. Levitt, P. M. Thompson, et al. // Psychiatry Research, vol. 107(1), p. 29–43, 2001.
18. Iftekharuddin K. M. Fractal analysis of tumor in brain MR images. / K. M Iftekharuddin, Jia W, Marsh R. // Machine Vision and Applications, vol.13(5-6), p. 352–362, 2003.
19. Liu Jing Z. Fractal Dimension in Human Cerebellum Measured by Magnetic Resonance Imaging. / Jing Z. Liu, Lu D. Zhang, Guang H. Yue // Biophysical Journal vol. 85, p. 4041–4046, 2003.
20. Lee Jong-Min. Analysis of the hemispheric asymmetry using fractal dimension of a Skeletonized Cerebral Surface. / Jong-Min Lee, Uicheul Yoon, Jae-Jin Kim, et al. // IEEE Transactions on Biomedical Engineering, vol. 51 (8), p. 1494–1998, 2004.
21. Mandelbrot B. B. The fractal geometry of nature. / B. B. Mandelbrot; Freeman, New York, 1982, ISBN 0-7167-1186-9.
22. Falconer K. J. Fractal geometry: mathematical foundations and applications. / K. J. Falconer; New York, John Wiley&Sons, 1990. ISBN-10: 0471922870
23. Feder J. Fractals. / J. Feder; Plenum Press, New York, 1988. ISBN 0-306-42851-2
24. Crownover R. M. Introduction to fractals and chaos. / R. M. Crownover; Jones and Bartlett Publishers Inc., 1995, ISBN 0867204648
25. Peitgen H. Chaos and fractals: new frontiers of science. / H. Peitgen, Jurgens H., Saupe D.; Springer-Verlag, New York, 1992, ISBN: 3540979034
26. Schroeder M. Fractals, chaos, power laws: minutes from an infinite paradise. /M. Schroeder; Freeman, New York, 1991. ISBN-10: 0716723573
27. Gouyet J.F. Physics and fractal structures. /J. F. Gouyet; Springer-Verlag, Masson, 1996. ISBN 0-387-94153-1
28. Kindratenko V. Development and application of image analysis techniques for identification and classification of microscopic particles. / V. Kindratenko; Universiteit Antwerpen, Ph.D. Thesis, Antwerpen, 1997.

Бучко О. А.

КЛАСИФІКАЦІЯ РАДІОЛОГІЧНИХ ЗОБРАЖЕНЬ НА ОСНОВІ АНАЛІЗУ ФОРМИ ОБ'ЄКТІВ

Розглянуто результати дослідження застосування методів опису форми об'єктів для класифікації нормальних і патологічних структур мозку в зображеннях магнетичного резонансу. Методи опису форми застосовано до двох груп: до першої групи ввійшли 30 здорових людей, до другої – 17 пацієнтів з патологією мозку.